JOURNAL OF Materials CHEMISTRY

New cation conducting solid electrolytes with the $Sc_2(WO_4)_3$ type structure

Joachim Köhler, Nobuhito Imanaka and Gin-ya Adachi*

Department of Applied Chemistry, Faculty of Engineering, Osaka University, 2–1 Yamadaoka, Suita, Osaka 565–0871, Japan. E-mail: adachi@chem.eng.osaka-u.ac.jp

Received 5th February 1999, Accepted 22nd March 1999

The $Sc_2(WO_4)_3$ type structure has been used in order to create new trivalent cation conducting solid electrolytes by forming solid solutions of the type $(Sc_2(WO_4)_3)_{1-x}(M_2(MoO_4)_3)_x$ (M = Nd, Sm, Gd, Lu). In these compounds, the anionic part of the structure is partly replaced by molybdate ($WO_4 \rightarrow MoO_4$) whereas the Sc^{3+} cations are substituted by different larger lanthanide cations M (Sc→M). Increasing the size of M gradually leads to a restriction of the $M_2(WO_4)_3$ solubility in the scandium tungstate phase (*e.g.*, $x = 0$–1 for M = Lu but $x = 0$–0.1 for M = Nd). The electrical properties of the resulting materials have been characterized in detail. All solid solutions exhibit neither electronic nor anionic O^{2-} conduction but rather a mixed trivalent Sc^{3+}/M^{3+} cationic conduction with the Sc^{3+} cations as the main charge carrying species for low $M_2(MoO_4)_3$ concentrations ($x < 0.5$) and the ionic transference number is >99%. For a given substitution rate of M for Sc, the electrical conductivity increases with increasing size of M. The highest conduction data were observed for the solid solution $(Sc_2(WO_4)_3)_{0.75}(Sm_2(MoO_4)_3)_{0.25}$ exhibiting a conductivity of 2.4×10^{-4} S cm^{-1} at 600 °C with an activation energy of 45.8 kJ mol^{-1}. Furthermore, in all different systems the maximum conductivity appears for the same average trivalent cationic radius indicating an optimized spatial spacing for the mobile cationic species.

1 Introduction

One of the main research topics in solid state ionics is the creation of new ion conducting compounds which can be used as solid electrolyte materials in technical applications, such as *e.g.* batteries, sensors, *etc.* Usually, already known materials with known physical properties are chemically altered in order to obtain compounds with better physical characteristics. Scandium tungstate, $Sc_2(WO_4)_3$, appears to be an excellent candidate material for this method. Its electrochemical properties, especially the trivalent cation conducting characteristics, are already well established[1–5] and it is possible to chemically substitute the anionic host lattice as well as the mobile trivalent cation to synthesize new types of cation conductors.

The crystal structure of $Sc_2(WO_4)_3$ [in general $M_2(WO_4)_3$] consists of a three-dimensional network of $[M_2W_3O_{18}]$ units built up by MO_6 octahedra and WO_4 tetrahedra. This building principle can also be found in the crystal structures of the fast Li^+ or Na^+ conducting γ-$Li_3Sc_2(PO_4)_3$[6] or NASICON[7] compounds. In all these structure types the mobile cations are assumed to move through open tunnels or layers. Considering $M_2(WO_4)_3$, M can be represented by trivalent cations of the smaller rare earth metals Gd–Lu, Sc or by trivalent cations of the main group elements In and Al.[8] Corresponding molybdates with this structure type are formed by Ho–Lu, Sc, In and Al.[8] Among the tungstates, $Al_2(WO_4)_3$ exhibits the lowest ($\sigma = 3.4 \times 10^{-6}$ S cm^{-1} at 600 °C) and $Sc_2(WO_4)_3$ the highest ($\sigma_{600\,°C} = 3.7$–6.5×10^{-5} S cm^{-1}, depending on the sintering temperature) electrical conduction properties.[9] Considering the isotypic molybdates which contain the same mobile species M, the electrical conductivity in $M_2(MoO_4)_3$ is always higher than in the corresponding tungstates $M_2(WO_4)_3$ [*e.g.* $Sc_2(WO_4)_3$: $\sigma_{600\,°C} = 6.5 \times 10^{-5}$ S cm^{-1} and $Sc_2(MoO_4)_3$: $\sigma_{600\,°C} = 9.0 \times 10^{-5}$ S cm^{-1}].[9] This behavior is caused by a higher mobility of the migrating cations due to reduced Columbic interactions with the oxygen anions of the surrounding MoO_4^{2-} groups (shorter Mo–O distances, in comparison to W–O in tungstate compounds).

Recently, solid solutions in the tungstate–tungstate systems $(Al_2(WO_4)_3)_{1-x}(Sc_2(WO_4)_3)_x$,[10] $(Sc_2(WO_4)_3)_{1-x}(Lu_2(WO_4)_3)_x$,[9,11] and $(Sc_2(WO_4)_3)_{1-x}(Gd_2(WO_4)_3)_x$[12] have been reported in which the cationic conductivity is increased in comparison to the undoped $Al_2(WO_4)_3$ (by about six times) and $Sc_2(WO_4)_3$ (by about two and three times, respectively). In these compounds, the Sc site is partially replaced with larger M cations (radius $r_{M^{3+}} > r_{Sc^{3+}}$) which act to enlarge the migration pathways enabling smoother movement of the mobile cations.

In contrast to these experiments, we report here on the electrical characteristics of $Sc_2(WO_4)_3$ derivatives in which both the cationic and the anionic part of the crystal structure have been altered. With respect to the higher electrical conduction properties of the molybdate compounds, the corresponding $M_2(MoO_4)_3$ has been used to form solid solutions in the systems $(Sc_2(WO_4)_3)_{1-x}(M_2(MoO_4)_3)_x$ (M = Nd, Sm, Gd, Lu). In these materials, not only is Sc^{3+} is replaced by larger M^{3+} cations but also MoO_4^{2-} is substituted for WO_4^{2-} in order to combine the conductivity enhancement by the M-spacing effect with the increased conduction properties of the molybdate compounds. Higher electrical conductivity data are expected for these tungstate–molybdate solid solutions in comparison to the tungstate–tungstate ones.

2 Experimental

Solid solutions of $(Sc_2(WO_4)_3)_{1-x}(M_2(MoO_4)_3)_x$ (M = Nd, Sm, Gd, Lu) in a polycrystalline state were prepared in conventional solid state reactions by heating a thoroughly ground mixture of reagent grade Sc_2O_3, WO_3, MoO_3, and the lanthanide oxides M_2O_3 (purity of all reagents ≥99.9%) in the corresponding stoichiometric ratio at a temperature below 800 °C for 12–24 h in an oxygen atmosphere. This low reaction temperature during the first heating cycle was used in order to avoid the loss of MoO_3 which melts at *ca.* 795 °C. During this procedure, MoO_3 has chemically reacted to form either already the expected tungstate–molybdate solid solutions or

mixtures of single tungstate and molybdate compounds. Those molybdates are thermally more stable to the loss of MoO_3 and the temperature could be raised to 1000–1100 °C (12–24 h) in a second heating cycle (after regrinding) in order to finally complete the synthesis of the solid solutions. The obtained powders are white (Sc/Lu and Sc/Gd compounds), salmon-pink (Sc/Sm), and violet (Sc/Nd). The resulting white polycrystalline materials were characterized by X-ray powder diffraction analysis (XRD) using Cu-Kα radiation (Mac Science M18XHF diffractometer).

For the electrical measurements, pelletized samples of $(Sc_2(WO_4)_3)_{1-x}(M_2(MoO_4)_3)_x$ were sintered in oxygen atmosphere for 12 h at 1200 °C (M = Lu, Gd) or 1100 °C (M = Sm, Nd), and sputtered on opposite faces with ionically blocking platinum. Electrical measurements by complex impedance analysis were obtained at temperatures between 200 and 700 °C within the frequency range 20 Hz–1 MHz (Hewlett-Packard precision LCR meter, 8284A). Time-dependent dc-polarization measurements were performed by passing a constant direct current ($I_{dc} = 1$ μA) through the sample and monitoring the terminal dc voltage (V_{dc}) as a function of time in atmospheres of oxygen ($P_{O_2} = 1 \times 10^5$ Pa), nitrogen ($P_{O_2} = 10^2$ Pa) and helium ($P_{O_2} = 4$ Pa), respectively.

For dc electrolysis experiments, the samples were placed between two Pt-plates as ion-blocking electrodes and exposed to a direct voltage of 6 V for *ca.* 4–6 weeks at 800–850 °C in air atmosphere. After the electrolysis procedure, the cathodic and anodic surfaces of the samples were characterized by X-ray powder diffraction (XRD) and by EPMA. For measuring a cross-sectional EPMA line analysis, the electrolyzed pellet was fixed within an epoxy resin, cut perpendicular to the plate area (anode to cathode direction) and polished with diamond paste (average diameter 0.5 μm).

3 Results and discussion

3.1 Characterization

The amount (x) of $M_2(MoO_4)_3$ which can be dissolved in $Sc_2(WO_4)_3$ to form the $(Sc_2(WO_4)_3)_{1-x}(M_2(MoO_4)_3)_x$ solid solutions strongly depends on the cationic radius of M. This behavior is shown in Fig. 1 where the highest amount (x_{max}) of $M_2(MoO_4)_3$ dissolved is given as a function of the ionic radii of M (normalized by the ratio $r_{M^{3+}}/r_{Sc^{3+}}$; the radii are taken from ref. 13) and the composition of the solid solution. Considering the investigated systems, a complete solid solution over the whole composition range is only possible for the $(Sc_2(WO_4)_3)_{1-x}(Lu_2(MoO_4)_3)_x$ systems. With increasing size of M ($r_{M^{3+}} > r_{Lu^{3+}}$) the solubility of $M_2(MoO_4)_3$ in the tungstate is drastically reduced down to $x = 0.1$ for M = Nd while $La_2(MoO_4)_3$ can not be incorporated into $Sc_2(WO_4)_3$ at all. Attempts to prepare $(Sc_2(WO_4)_3)_{1-x}(M_2(MoO_4)_3)_x$ solid solutions with $r_{M^{3+}}/r_{Sc^{3+}} > x_{max}$ (open circles in Fig. 1) always led to the formation of two phase systems consisting of the corresponding tungstate and molybdate compounds.

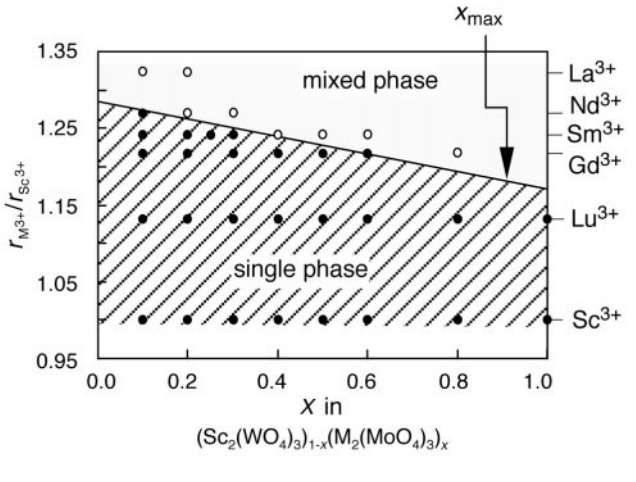

Fig. 1 Range of solubility of $M_2(MoO_4)_3$ (M = La, Nd, Sm, Gd, Lu) in $Sc_2(WO_4)_3$ in relation to the cationic radius of M (expressed as $r_{M^{3+}}/r_{Sc^{3+}}$). The solid line represents the phase limits, x_{max}, for the $(Sc_2(WO_4)_3)_{1-x}(M_2(MoO_4)_3)_x$ (M = La, Nd, Sm, Gd, Lu) systems. (●) corresponds to the formation of single phase $(Sc_2(WO_4)_3)_{1-x}(M_2(MoO_4)_3)_x$ solid solutions whereas (○) denotes the formation of a mixture of tungstates and molybdates, respectively.

It is interesting that the pure molybdates $M_2(MoO_4)_3$ (M = Nd, Sm, or Gd) do not adopt the $Sc_2(WO_4)_3$ type structure but rather crystallize in the different $Eu_2(WO_4)_3$ structure type[8] which is not appropriate for cationic migration. Thus, these molybdates behave as insulators. However, the cation conducting $Sc_2(WO_4)_3$ type structure tolerates a size mismatch of the trivalent cation to a certain extent and by the formation of the $(Sc_2(WO_4)_3)_{1-x}(M_2(MoO_4)_3)_x$ solid solutions it becomes possible to create new type of electrolyte materials.

3.2 Electrical properties

The conductivity data as well as the activation energies of the $(Sc_2(WO_4)_3)_{1-x}(M_2(MoO_4)_3)_x$ solid solutions (M = Nd, Sm, Gd, Lu) are summarized in Table 1. In addition, these data are compared to the average trivalent cationic radius (r_m) of each compound [$r_m = (1-x)\, r_{Sc^{3+}} + x r_{M^{3+}}$; the radii are taken from ref. 13]. Because the ionic radii of W^{6+} (0.056 nm[13]) and Mo^{6+} (0.055 nm[13]) are almost identical, the extension of the crystallographic unit cell in these compounds mainly depends on the ionic radius of the trivalent cations. The incorporation of larger cations in $Sc_2(WO_4)_3$ ($r_{M^{3+}} > r_{Sc^{3+}}$) leads to a linear expansion of the unit cell dimensions as indicated by a corresponding shifted d-spacing of individual peaks in the XRD pattern. The resulting opened pathways within the crystal structure reduce the electrostatic interactions between the mobile cations and the anionic host lattice leading to increased mobilities. This is shown in Fig. 2, where the electrical conductivities ($\log \sigma$) of different $(Sc_2(WO_4)_3)_{0.9}(M_2(MoO_4)_3)_{0.1}$ (M = Nd, Sm, Gd, Lu) solid solutions with a fixed composition ($x = 0.1$) at 600 °C are plotted *vs.* the cationic radius of M. By substituting the Sc site with larger M cations, the conductivity continuously increases up to 2.3×10^{-4} S cm^{-1} in $(Sc_2(WO_4)_3)_{0.9}(Nd_2(MoO_4)_3)_{0.1}$ which represents one of the highest values among the various investigated $(Sc_2(WO_4)_3)_{1-x}(M_2(MoO_4)_3)_x$ solid solutions.

Considering a given $(Sc_2(WO_4)_3)_{1-x}(M_2(MoO_4)_3)_x$ system with a given cation M, the electrical conductivity exhibits a more complex behavior *vs.* $M_2(MoO_4)_3$ content x, as shown in Fig. 3(a). Starting from pure $Sc_2(WO_4)_3$, the conductivity continuously increases with x owing to opened migration pathways by the incorporation of the larger cation M. However, at a given composition, the conductivity reaches a maximum and the addition of further $M_2(MoO_4)_3$ reduces the conduction properties. This behavior is assumed to be due to the presence of different trivalent cations with different migration properties. Recently, it was shown that Sc^{3+} cations are the most suitable and appropriate charge carriers in tungstates and molybdates of $Sc_2(WO_4)_3$ type structure.[5,9] Thus, it is assumed that in the $(Sc_2(WO_4)_3)_{1-x}(M_2(MoO_4)_3)_x$ solid solutions with a low $M_2(MoO_4)_3$ concentration Sc^{3+} cations represent the main mobile charge carriers whose conduction properties are enhanced by the spacing effect of the larger M cations. However, with increasing content of $M_2(MoO_4)_3$ the number of highly mobile Sc^{3+} cations diminishes and the fraction of larger and less mobile M cations increases which finally causes a fall in conductivity. This interpretation is supported by results from dc electrolysis experiments on various $(Sc_2(WO_4)_3)_{1-x}(M_2(MoO_4)_3)_x$ com-

Table 1 Comparison of the electrical conductivity data (upper row: log $\sigma_{600\,^\circ C}$) and the corresponding activation energies E_a (lower row: temperature range 400–700 °C) of the investigated $(Sc_2(WO_4)_3)_{1-x}(M_2(MoO_4)_3)_x$ solid solution compounds. The average trivalent cationic radius ($r_m=(1-x)r_{Sc^{3+}}+xr_{M^{3+}}$) is shown in the middle row. Italicised data do not belong to compounds of the $Sc_2(WO_4)_3$ type structures[a]

Upper row: conductivity at 600 °C (log σ)
Middle row: average cationic radius/nm
Lower row: activation energy/kJ mol^{-1}

$Sc_2(WO_4)_3$: log $\sigma_{600\,^\circ C}=-4.427$
$r_{Sc^{3+}}=0.0885$ nm
$E_a=44.1$ kJ mol^{-1}

M/x	0.10	0.20	0.25	0.30	0.40	0.50	0.60	0.80	1.00
Lu	−4.268	−4.149		−4.065	−3.931	−3.921	−4.053	−4.167	−4.225
	0.0897	0.0908		0.0920	0.0931	0.0943	0.0955	0.0978	0.1001
	47.7	46.0		46.0	47.9	49.1	47.7	46.4	39.2
Gd	−4.133	−3.953		−3.905	−3.956	−4.203	−4.3029	—[a]	*−6.354*
	0.0904	0.0924		0.0943	0.0962	0.0982	0.1008		*0.1078*
	48.8	44.9		45.1	48.2	42.3	43.2		*94.7*
Sm	−3.877	−3.777	−3.628	−3.752	−4.4926	—[a]	—[a]	—[a]	*−6.478*
	0.0906	0.0928	0.0938	0.0949	0.0970				*0.1098*
	47.8	47.6	45.8	45.2	49.8				*144.8*
Nd	−3.631	—[a]	—[a]	—[a]	—[a]	—[a]	—[a]	—[a]	*−6.139*
	0.0909								*0.1123*
	46.9								*112.4*

[a]Solid solution not formed.

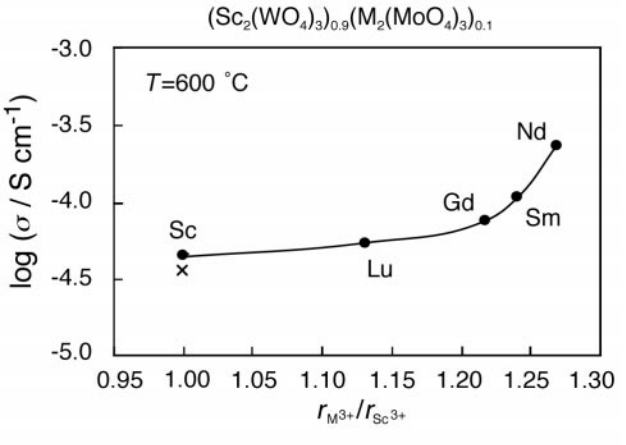

Fig. 2 Electrical conductivity (log σ) of $(Sc_2(WO_4)_3)_{0.9}$-$(M_2(MoO_4)_3)_{0.1}$ (M = Nd, Sm, Gd, Lu, Sc) solid solutions at 600 °C in relation to the cationic radius of M (expressed as $r_{M^{3+}}/r_{Sc^{3+}}$). The conductivity of pure $Sc_2(WO_4)_3$ is denoted by ×.

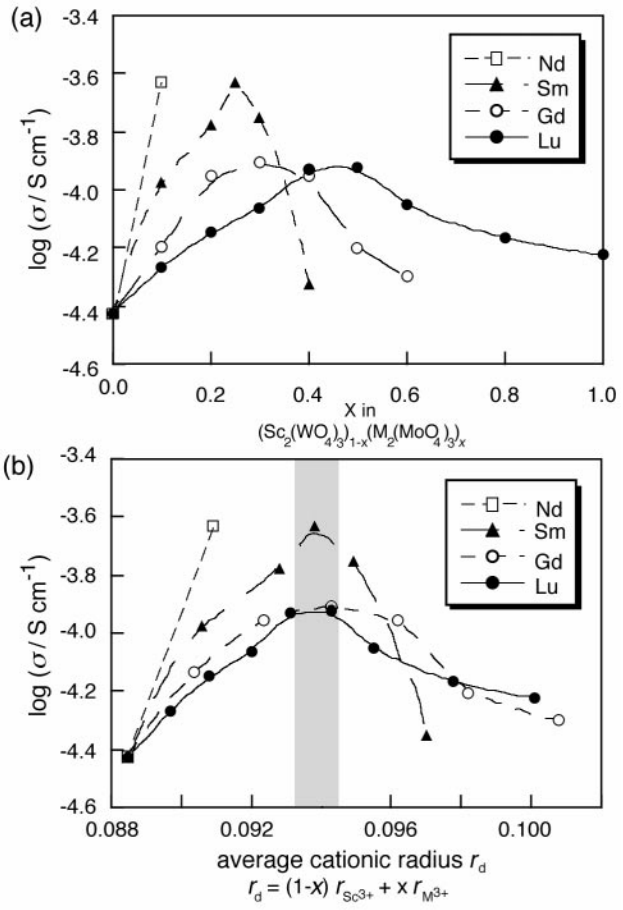

Fig. 3 The electrical conductivity (log σ) of $(Sc_2(WO_4)_3)_{1-x}(M_2(MoO_4)_3)_x$ [M = Nd (□), Sm (▲), Gd (○), Lu (●)] solid solutions at 600 °C (a) *vs.* the $M_2(MoO_4)_3$ content, x and (b) *vs.* the average trivalent cationic radius, r_d. The shaded region in (b) corresponds to the optimal cationic radius where the highest conductivity data has been observed.

pounds where the migrating cations are directly identified. These results will be given in the subsequent sections. Pure $Nd_2(MoO_4)_3$, $Sm_2(MoO_4)_3$ and $Gd_2(MoO_4)_3$ crystallize in a crystal structure which is different from the $Sc_2(WO_4)_3$ structure type[8] and which is not appropriate for conducting cations as can be seen from their comparatively low conductivities (Table 1). These data do not correspond to the conduction characteristics of the $Sc_2(WO_4)_3$ type structure but are simply given for comparison.

Table 1 indicates another interesting feature which is shown in Fig. 3(b). The maximum value of electrical conduction in the $(Sc_2(WO_4)_3)_{1-x}(M_2(MoO_4)_3)_x$ systems is observed for an average cationic radius of *ca.* 0.0938–0.0943 nm. In this context it is interesting that in the tungstate–tungstate systems the maximum enhancement effect on the conductivity is also observed for compositions corresponding to this average trivalent cationic radius. These observations imply that (i) the molybdenum ions do not significantly influence the spatial conditions of the migration pathways and (ii) the $Sc_2(WO_4)_3$ type structure possesses a certain spatial spacing of the migration pathways, which is most appropriate for the transport of the trivalent Sc^{3+} cations. According to this assumption, the highest conductivity in the $(Sc_2(WO_4)_3)_{1-x}$-$(Nd_2(MoO_4)_3)_x$ system is expected for the compound corresponding to a composition with $x=0.2$–0.25. However, owing to the limited solid solution range, this maximum could not be achieved. Nevertheless, this information for the optimized pathway extension is valuable for a future tailoring of new solid electrolytes with the $Sc_2(WO_4)_3$ type structure. The composition and thus the spatial properties can be adjusted

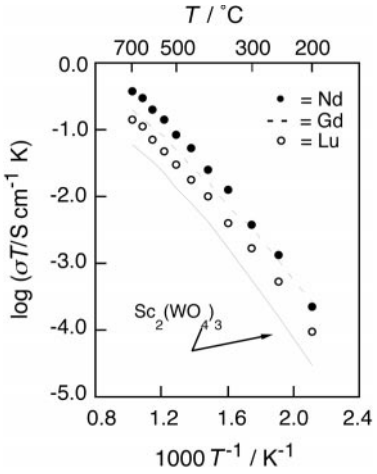

Fig. 4 Temperature dependencies of the electrical conductivity of $Sc_2(WO_4)_3$ (—), $(Sc_2(WO_4)_3)_{0.5}(Lu_2(MoO_4)_3)_{0.5}$ (○), $(Sc_2(WO_4)_3)_{0.7}(Gd_2(MoO_4)_3)_{0.3}$ (----) and $(Sc_2(WO_4)_3)_{0.9}$-$(Nd_2(MoO_4)_3)_{0.1}$ (●).

in order to find the optimum composition for the highest conduction characteristics.

The activation energies, E_a, for the $(Sc_2(WO_4)_3)_{1-x}$-$(M_2(MoO_4)_3)_x$ compounds are calculated from the corresponding Arrhenius diagram within the temperature range 400–700 °C where the experimental data could be adequately fitted by a linear regression. Some representative Arrhenius plots of the highest conducting compound in each system (for a given M cation) are given in Fig. 4. All other investigated $(Sc_2(WO_4)_3)_{1-x}(M_2(MoO_4)_3)_x$ solid solutions exhibit a similar behavior and the activation energies in the high temperature range ($T > 400$ °C) amount to 43.5–49.7 kJ mol^{-1}, similar to the data of pure $Sc_2(WO_4)_3$ ($E_a = 44.1$ kJ mol^{-1}).

With respect to solid solutions in the tungstate–tungstate systems $(Sc_2(WO_4)_3)_{1-x}(Lu_2(WO_4)_3)_x$[9,11] and $(Sc_2(WO_4)_3)_{1-x}(Gd_2(WO_4)_3)_x$[12] it can be stated that the conductivity enhancement in the tungstate–molybdate systems is not only caused by the incorporation of larger cations at the Sc site but is also influenced by the Mo ions in the anionic host lattice. For example, the electrical conductivity in $(Sc_2(WO_4)_3)_{0.5}(Lu_2(MoO_4)_3)_{0.5}$ ($\sigma_{600\,°C} = 2.3 \times 10^{-4}$ S cm^{-1}) and $(Sc_2(WO_4)_3)_{0.7}(Gd_2(MoO_4)_3)_{0.3}$ ($\sigma_{600\,°C} = 3.5 \times 10^{-4}$ S cm^{-1}) compounds is remarkably higher than in the corresponding $(Sc_2(WO_4)_3)_{0.5}(Lu_2(WO_4)_3)_{0.5}$ ($\sigma_{600\,°C} = 4.0 \times 10^{-5}$ S cm^{-1})[11] and $(Sc_2(WO_4)_3)_{0.7}(Gd_2(WO_4)_3)_{0.3}$ ($\sigma_{600\,°C} = 6.2 \times 10^{-5}$ S cm^{-1})[12] solid solutions where only the Sc site has been substituted. The difference between these two distinct systems (tungstate–molybdate *cf.* tungstate–tungstate) reflects the influence of the slightly smaller Mo atoms. The lattice parameters in the molybdate compounds are reduced in comparison to the homologous tungstates [*e.g.* $Sc_2(WO_4)_3$: $a = 0.9669$, $b = 1.3327$, $c = 0.9581$ nm and $Sc_2(MoO_4)_3$: $a = 0.9656$, $b = 1.327$, $c = 0.9563$ nm).[14] As a result, the Mo–O distances are shortened and the negative charge density of the oxide anions in the MoO_4^{2-} groups is lowered, in comparison to that of the oxide anions in the corresponding WO_4^{2-} groups. Thus, the Coulomb interactions to the migrating trivalent cations are reduced leading to increased mobilities and more enhanced conductivities in the molybdate containing compounds.

It is evident that the electrical conduction in $(Sc_2(WO_4)_3)_{1-x}(M_2(MoO_4)_3)_x$ solid solutions (M = Nd, Sm, Gd, Lu) is improved with respect to pure $Sc_2(WO_4)_3$ as well solid solutions in the tungstate–tungstate systems $(Sc_2(WO_4)_3)_{1-x}(M_2(WO_4)_3)_x$ (M = Gd, Lu).[11,12] This enhancement is due to (i) the opening of the migration pathways by the incorporation of larger Sc^{3+} cations and (ii) reduced anionic lattice–mobile cation interactions by the incorporation of molybdate groups. The molybdate groups within the anionic host lattice do not significantly influence the steric condition for the migrating cations but rather induce a changed electrostatic situation.

To characterize the electrical conduction in the $(Sc_2(WO_4)_3)_{1-x}(M_2(MoO_4)_3)_x$ solid solutions (M = Nd, Sm, Gd, Lu) in more detail and especially to characterize the mobile charge carrying species, various electrical measurements have been performed. The procedure for performing the polarization measurements to estimate the dc conductivity has already been described elsewhere and will not be reported here.[1–5] As a result, the dc conductivity which is originated solely by the transport of electronic charge carriers (within the used experimental setup) is *ca.* two to three orders of magnitude lower in comparison to the ac conductivity (σ_{ac} as measured by impedance spectroscopy is composed of ionic and electronic conduction). Thus, the electrical conductivity in the solid solutions is purely ionic with ion transference numbers higher than $t_i = 0.99$. In order to investigate the possibility of anionic O^{2-} conduction, the dc and ac conductivities were measured in various atmospheres, differing in oxygen partial pressure [*e.g.*, oxygen ($P_{O_2} = 10^5$ Pa), nitrogen ($P_{O_2} = 10^2$ Pa) and helium ($P_{O_2} = 4$ Pa)]. However, no alterations of the conductivity data were observed by changing the atmosphere. This observation indicates that the ionic conduction in $(Sc_2(WO_4)_3)_{1-x}(M_2(MoO_4)_3)_x$ is not of O^{2-} anionic origin but in turn must be generated by the migration of cations. If O^{2-} anions were the main mobile charge carriers, the conductivity should be dependent on the oxygen partial pressure. All of these observations are in accord with the results of corresponding experiments in other trivalent cationic conducting compounds of the $Sc_2(WO_4)_3$ type structure.[1–5,9–12]

3.3 Electrolysis

The remaining question concerns the identification of the migrating cations in $(Sc_2(WO_4)_3)_{1-x}(M_2(MoO_4)_3)_x$, *i.e.* which of the present trivalent cations, Sc^{3+} or M^{3+}, is mobile. To elucidate this matter, dc electrolysis experiments have been performed on various samples differing in $M_2(MoO_4)_3$. In all cases, white precipitates were observed on the cathodic surface as well as on the Pt-cathode after the electrolysis. Single deposits within these cathodic precipitations were qualitatively and quantitatively analyzed by EPMA and found to consist of the elements scandium, tungsten (molybdenum) and M. In Table 2, some representative results of these EPMA measure-

Table 2 Comparison of the surface composition of some selected $(Sc_2(WO_4)_3)_{1-x}(M_2(MoO_4)_3)_x$ (M = Lu, Gd, Sm, Nd) solid solution samples before and after dc electrolysis, according to EPMA measurements

	Before electrolysis (atom%)				After electrolysis (atom%)			
Compound	Sc	M	W	Mo	Sc	M	W	Mo
$(Sc_2(WO_4)_3)_{0.5}(Lu_2(MoO_4)_3)_{0.5}$	20	20	30	30	28.9	24.8	28.4	17.9
$(Sc_2(WO_4)_3)_{0.7}(Gd_2(MoO_4)_3)_{0.3}$	28	12	42	18	33.2	13.8	39.7	13.3
$(Sc_2(WO_4)_3)_{0.75}(Sm_2(MoO_4)_3)_{0.25}$	30	10	45	15	39.1	12.5	40.3	8.9
$(Sc_2(WO_4)_3)_{0.9}(Nd_2(MoO_4)_3)_{0.1}$	36	4	54	6	60.9	6.6	27.1	5.4

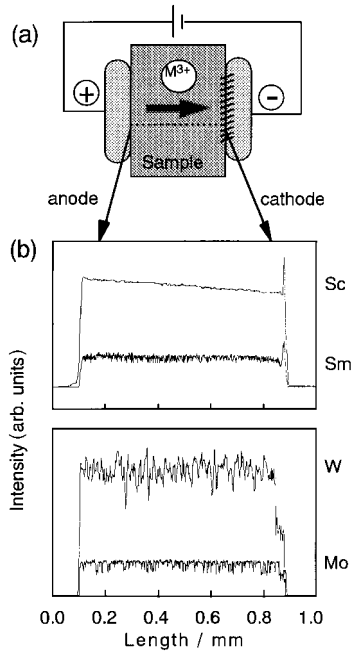

Fig. 5 (a) Schematic representation of the electrolysis cell and (b) the cross sectional EPMA line analysis [indicated by the broken line in (a)] for the elements scandium, samarium, tungsten and molybdenum after electrolysis of $(Sc_2(WO_4)_3)_{0.75}(Sm_2(MoO_4)_3)_{0.25}$.

ments are given, as observed on the cathodic surfaces of the samples before and after the electrolysis procedure. It can be seen that both the Sc/W (Sc/Mo) and the M/W (M/Mo) atomic ratio are increased with regard to the composition before the electrolysis. Furthermore, the concentration of Sc has been raised in comparison to the M content (increased Sc/M ratio after the electrolysis). Also on the anodic surface of the electrolyzed pellets the color changed to yellow–green after electrolysis indicating the formation of WO_3. This assumption was verified by EPMA measurements where the corresponding colored particles are found to consist only of tungsten (WO_3). Corresponding particles containing molybdenum (indicating the formation of MoO_3) were not observed. MoO_3 sublimes at *ca.* 800 °C and due to the high electrolysis temperature (800–850 °C) any formed molybdenum oxide would instantly evaporate from the anionic sample surfaces. However, at cooler parts of the furnace which were used for the electrolysis procedures, the evaporated MoO_3 precipitated in the form of needle shaped crystals which could be clearly identified by X-ray powder diffraction analysis.

Besides the characterization of the sample surfaces, the Sc, M and W(Mo) distributions within the bulk of the same electrolyzed samples were also determined by EPMA measurements by performing cross-sectional area (perpendicular to the platelet area) analyses. As an example, the integrated intensities as measured for the elements scandium, samarium and tungsten(molybdenum) in the solid solution with the composition $Sc_2(WO_4)_3)_{0.75}(Sm_2(MoO_4)_3)_{0.25}$ are shown in Fig. 5. Within the bulk, scandium, samarium and tungsten (molybdenum) are equally distributed whereas at the cathodic side of the pellet a sudden increase of Sc and Sm as well as a decrease of the W (Mo) content can be observed. Similar results have been obtained for corresponding EPMA measurements of other $Sc_2(WO_4)_3)_{1-x}(M_2(MoO_4)_3)_x$ solid solutions.

All the observations from the various electrolysis experiments can be explained by assuming the $Sc_2(WO_4)_3)_{1-x}(M_2(MoO_4)_3)_x$ solid solutions as mixed cationic conductors with trivalent Sc^{3+} and M^{3+} cations as mobile species. During electrolysis, the cations migrate from the anodic side of the pellet through the bulk toward the Pt-cathode where a chemical reaction (with the surrounding tungstate matrix and the atmospheric oxygen) occurs. As a result, the trivalent cations accumulate at the cathode and at the anodic side pure WO_3 remains. Furthermore, comparing the mobility of the different rare earth cations, the Sc^{3+} cations appear to move more easily than the corresponding larger cations and represent the main mobile species in these compounds. Especially in the case of $Sc_2(WO_4)_3)_{0.9}$-$(Nd_2(MoO_4)_3)_{0.1}$, the Sc^{3+} content is significantly increased indicating its promoted migration properties. The larger M^{3+} cations are sterically more hindered for a smooth ion transport and act to expand the crystal lattice for easier transport of the Sc^{3+} cations. This assumption explains (i) the similar activation energies which are comparable to those of pure $Sc_2(WO_4)_3$ and (ii) the increased Sc : M atomic ratio on the cathodic surfaces after the electrolysis (see Table 2). However, it must be emphasised that the larger lanthanide cations Lu^{3+}, Gd^{3+}, Sm^{3+} and even Nd^{3+} are also mobile to a certain extent as indicated in Table 2 by the raised M/W (M/Mo) atomic ratios. Thus, these $Sc_2(WO_4)_3)_{1-x}(M_2(MoO_4)_3)_x$ solid solutions are the first compounds for which the migration of large trivalent cations (*e.g.* Gd^{3+}, Sm^{3+}, Nd^{3+}) has been demonstrated for the first time.

4 Conclusion

Solid solutions in the systems $(Sc_2(WO_4)_3)_{1-x}(M_2(MoO_4)_3)_x$ (M = Nd, Sm, Gd, Lu) have been shown to be pure cationic conductors exhibiting no oxide anionic or electronic conduction. Considering the cationic conduction, both Sc^{3+} and M^{3+} cations are mobile but Sc^{3+} migration dominates for compounds with comparatively low $M_2(MoO_4)_3$ content. The conduction properties are enhanced in comparison to pure $Sc_2(WO_4)_3$ due to the simultaneous effect of increasing the tunnel size for the ionic migration and reducing the electrostatic interactions between the anionic host lattice and mobile ions. Furthermore, a relationship between the conduction behavior and the trivalent cationic radius has been observed which is important for a tailoring of new solid electrolytes in the future, based on the $Sc_2(WO_4)_3$ type structure, with optimized conduction characteristics.

Acknowledgements

The present work was partially supported by a Grant-in-Aid for Scientific Research No. 09215223 on Priority Areas (No. 260), Nos. 06241106, 06241107, and 093065 from The Ministry of Education, Science, Sports and Culture. It was also supported by the 'Research for the Future, Preparation and Application of Newly Designed Solid Electrolytes (JSPS RFTF96P00102)' program from the Japan Society for the Promotion of Science (JSPS). J. K. gratefully acknowledges his postdoctoral fellowship for foreign researchers in Japan from the JSPS.

References

1 J. Köhler, N. Imanaka and G. Adachi, *Chem. Mater.*, 1998, **10**, 3790.
2 N. Imanaka, Y. Kobayashi and G. Adachi, *Chem. Lett.*, 1995, 433.
3 Y. Kobayashi, T. Egawa, S. Tamura, N. Imanaka and G. Adachi, *Chem. Mater.*, 1997, **9**, 1649.
4 N. Imanaka and G. Adachi, *J. Alloys Compd.*, 1997, **250**, 492.
5 N. Imanaka, Y. Kobayashi, K. Fujiwara, T. Asano, Y. Okazaki and G. Adachi, *Chem. Mater.*, 1998, **10**, 2006.
6 A. B. Bykov, A. P. Chipkin, L. N. Demyanets, S. N. Doromin, E. A. Genkina, A. K. Ivanov-Shits, I. P. Kondratyuk, B. A. Maksomov, O. K. Melnikov, L. N. Muradyan, V. I. Simonov and V. A. Timofeeva, *Solid State Ionics*, 1990, **38**, 31.
7 J. B. Goodenough, H. Y-P. Hong and J. A. Kafalas, *Mater. Res. Bull.*, 1976, **11**, 203.

8 K. Nassau, H. J. Levinstein and G. M. Loiacono, *J. Phys. Chem. Solids*, 1965, **26**, 1805.
9 Y. Kobayashi, PhD Thesis of Osaka University, 1998.
10 S. Tamura, T. Egawa, Y. Okazaki, Y. Kobayashi, N. Imanaka and G. Adachi, *Chem. Mater.*, 1998, **10**, 1958.
11 Y. Kobayashi, T. Egawa, S. Tamura, N. Imanaka and G. Adachi, *Solid State Ionics*, 1999, **118**, 325.
12 Y. Kobayashi, T. Egawa, S. Tamura, N. Imanaka and G. Adachi, *Solid State Ionics*, 1998, **111**, 59.
13 R. D. Shannon, *Acta Crystallogr., Sect. A*, 1976, **32**, 751.
14 A. W. Sleight and L. H. Brixner, *J. Solid State Chem.*, 1973, **7**, 172.

Paper 9/00999J